On the Calculation of Acyl Chain Order Parameters from Lipid Simulations

Thomas J. Piggot[1,2], Jane R. Allison[3], Richard B. Sessions[4] and Jonathan W. Essex[2]*

[1] Chemical, Biological and Radiological Sciences,
Defence Science and Technology Laboratory,
Porton Down,
Salisbury,
Wiltshire,
SP4 0JQ,
UK.

[2] Chemistry,
University of Southampton,
Highfield,
Southampton,
UK.

[3] Centre for Theoretical Chemistry and Physics,
Institute of Natural and Mathematical Sciences,
Massey University,
Auckland,
New Zealand.

[4] School of Biochemistry,
University of Bristol,
University Walk,
Bristol,
UK.

[*] Corresponding author. E-mail: tjpiggot@dstl.gov.uk and t.piggot@soton.ac.uk

Abstract

For molecular dynamics simulations of biological membrane systems to live up to the potential of providing accurate atomic level detail into membrane properties and functions, it is essential that the force fields used to model such systems are as accurate as possible. One membrane property that is often used to assess force field accuracy is the carbon-hydrogen (or carbon-deuterium) order parameters of the lipid tails, which can be accurately measured using experimental NMR techniques. There are a variety of analysis tools available to calculate these order parameters from simulations and it is essential that these computational tools work correctly to ensure the accurate assessment of the simulation force fields. In this work we compare many of these computational tools for calculating the order parameters of POPC membranes. While tools that work on all-atom systems and tools that work on saturated lipid tails in general work extremely well, we demonstrate that the majority of the tested tools that calculate the order parameters for unsaturated united-atom lipid tails do so incorrectly. We identify tools that do perform accurate calculations and include one such program with this work, enabling rapid and accurate calculation of united-atom lipid order parameters. Furthermore, we discuss cases in which it is non-trivial to appropriately predict the unsaturated carbon order parameters in united-atom systems. Finally, we examine order parameter splitting for carbon 2 in *sn*-2 lipid chains, demonstrating substantial deviations from experimental values in several all-atom and united-atom lipid force fields.

Introduction

Molecular dynamics simulations of phospholipid membranes have provided valuable atomic level details of many membrane processes over the past ~ 25 years, complementing more traditional wet-laboratory studies of such systems (e.g. [1-9] amongst many others). However, there are several limitations associated with these simulations that not only need to be understood to ensure careful interpretation of results, but are also areas in which advances must continue to be made to improve the accuracy and reliability of such computational work. These limitations include the ability of the simulation force fields to faithfully reproduce known experimental properties and the ability to sample enough of the conformational space of a given system to ensure converged results, amongst other related issues [10-14]. The latter of these two problems is often addressed in membrane simulations by applying methods that reduce the number of particles within the system, either through the use of coarse-grained [15-22] or united-atom [1,23-35] lipid models. In a classical united-atom lipid model, all non-polar hydrogen atoms are combined with their neighbouring carbon atoms to form united-atom CH, CH_2 and CH_3 groups. This not only substantially reduces the numbers of atoms within an individual lipid (e.g. for the commonly studied phospholipid 1, 2-dipalmitoyl-*sn*-glycero-3-phosphocholine (DPPC) the number of atoms reduces from 130 to 50) but also dramatically reduces the number of pairwise lipid interactions that need to be calculated at each time step during the simulations.

The ability of atomistic lipid models to reproduce experimentally derived membrane properties has been assessed in several publications, showing that most force fields generally demonstrate a reasonable level of accuracy [7,36-42]. One of the most frequent properties used for comparison between simulation and experiment are the order parameters (S_{CH}) of the lipid acyl chain tails. These order parameters, either calculated using quadrupolar splitting measured from deuterium NMR experiments [43-45] or dipolar splitting measured using carbon-13 NMR experiments [46-48], provide information regarding both the overall order of the membrane and specific details of the conformations that the atoms within the lipid tails adopt. Moreover, these different experimental NMR techniques provide consistent results, indicating accurate experimental measurements of this lipid property; this is discussed in further detail elsewhere [41]. These factors make S_{CH} an important property to analyse when developing, validating and comparing lipid force fields.

In this work we revisit the calculation of lipid acyl chain S_{CH} from molecular dynamics simulations. In particular, we focus upon current commonly used methods for calculating S_{CH} for both saturated and unsaturated lipid tails through the analysis of 1-palmitoyl-2-oleoyl-*sn*-glycero-3-phosphocholine (POPC) membrane simulations. Through comparison with values computed from all-atom simulations, we demonstrate substantial errors in the majority of available tools used to calculate S_{CH} for unsaturated lipid tails in united-atom systems. These problems extend to errors in the analysis method employed in the extensive set of simulations published by some of the authors of this publication [39] (referred to henceforth as the “previous comparative force field work”) and have, in some cases, resulted in incorrect

conclusions being drawn. Indeed, having re-calculated the S_{CH} from this previous comparative force field work using a tool that we validate herein, we have recently published a correction to some of the results of this previous work [49]. In this paper we also use validated tools to: further examine the unsaturated S_{CH} of the GROMOS 43A1-S3 united-atom force field [29]; assess united-atom force fields not included within our previous work; examine splitting of the S_{CH} for carbon 2 of the *sn*-2 lipid tails in both all-atom and united-atom systems. Finally, in providing a validated tool for both saturated and unsaturated united-atom lipid tail order parameter analysis, we hope to help guide the correct and rapid future analysis of such united-atom membrane systems.

Methods

Calculating Order Parameters from Simulations

To calculate the lipid acyl chain S_{CH} from an all-atom membrane simulation is a relatively simple task, given the explicit inclusion of all of the hydrogen atoms within the lipids. The calculation, as shown in Equation 1, describes the orientation of the C-H bond vector with respect to the bilayer normal (typically the *z* axis in a membrane simulation) averaged over all of the lipids and all of the sampling time [43,50].

$$S_{CH} = \langle 3cos^2\theta - 1\rangle/2 \qquad (1)$$

Equation 1 – Calculation of order parameters in all-atom systems. θ is the angle between the C-H bond vector and the bilayer normal. The angular brackets represent molecular and temporal ensemble averages.

There are many tools and programs available for performing such an analysis of S_{CH} in all-atom systems using Equation 1, several of which are described in more detail later in the methods. It is worth noting here that most of these analysis tools will automatically average the order parameters for the different hydrogen atoms attached to the same carbon atom. In most cases this makes little difference as rapid rotation around the normal to the H-C-H plane results in the experimental equivalence of the two order parameters [43,51]. However, there are some examples in which a splitting or forking (i.e. a difference in order parameters) does occur between such hydrogen atoms, for example at carbon 2 in phospholipid *sn*-2 chains [44,51]. In addition, taking such an averaging approach will also conceal any potential cancellation of errors in the simulations due to averaging.

In contrast to the all-atom systems, the calculation of S_{CH} from a united-atom membrane is more complex as the positions of the hydrogen atoms are not explicitly known. In the analysis of united-atom membrane simulations, S_{CH} are generally calculated using one of two closely related strategies. In one approach the calculation is explicitly broken down into two stages: the hydrogen positions are predicted and subsequently the S_{CH} are calculated in exactly the same manner as discussed for all-atom systems (Equation 1). This is the approach reported as being adopted in several

tools, as discussed in further detail below. In the second approach, thoroughly detailed in several previous works [1,24,50,52,53], the calculation of S_{CH} using predicted C-H bond vectors is performed in one single step. For methylene (i.e. CH_2) groups, the S_{CH} can be calculated using Equation 2.

$$S_{CH} = \frac{2}{3}S_{xx} + \frac{1}{3}S_{yy} \qquad (2)$$

Equation 2 – Calculation of saturated order parameters in united-atom systems using the one-step approach. S_{xx} and S_{yy} are the *xx* and *yy* axes order parameters with respect to the membrane normal, respectively. For example, $S_{xx} = \langle 3\cos^2\theta_x - 1\rangle/2$, where θ_x is the angle between the *x* axis and the membrane normal. This method requires the appropriate definition of the molecular frame of the system, as detailed in the text and shown in Figure 1 (left).

We stress here that Equation 2 relies upon the appropriate definition of the molecular frame of the system (Figure 1, left). If the methylene of interest is termed C_n, the *z* axis is defined as the C_{n-1} to C_{n+1} vector, the *x* axis is defined as perpendicular to the *z* axis (i.e. in the predicted H-C_n-H plane), and the *y* axis is perpendicular to both *x* and *z* axes (i.e. bisects the predicted H-C_n-H angle). This calculation also inherently assumes the equivalence of the two hydrogen atom order parameters. This does not have to be the case when taking this approach [52] but it is used in all of the available tools of which we are aware. For the calculation of the individual hydrogen atom order parameters in a united-atom methylene group, Equation 2 needs to be slightly modified as shown in Equations 3 and 4. As discussed later, we have implemented this approach for calculating the individual hydrogen atom order parameters in a modified version of the GROMACS program *g_order*.

$$S_{CH1} = \frac{2}{3}S_{xx} + \frac{1}{3}S_{yy} - \frac{2\sqrt{2}}{3}S_{xy} \qquad (3)$$

$$S_{CH2} = \frac{2}{3}S_{xx} + \frac{1}{3}S_{yy} + \frac{2\sqrt{2}}{3}S_{xy} \qquad (4)$$

Equations 3 and 4 – Calculation of the individual hydrogen atom order parameters in united-atom methylene groups using the one-step approach. S_{xx}, S_{yy} and S_{xy} are the *xx*, *yy* and *xy* axes order parameters with respect to the membrane normal. For example, $S_{xy} = \langle 3\cos\theta_x\cos\theta_y - 1\rangle/2$, where θ_x and θ_y are angles between *x* and *y* axes respectively and the membrane normal. This requires the same definition of the molecular frame of the system as in Equation 2. We note here that Equation 3 is slightly different to that reported by Douliez *et al.* [52] due to a typographical error in that work.

For methine (also termed methanylylidene) groups, as found within the carbon-carbon double bonds of unsaturated united-atom lipid tails, the calculation using this second approach is slightly more complex, as the terms of Equation 2 are reliant upon a

tetrahedral geometry. For this situation, the S_{CH} can be calculated using Equations 5 and 6.

$$S_n^{CH} = \frac{1}{4}S_{zz} + \frac{3}{4}S_{yy} - \frac{\sqrt{3}}{2}S_{yz} \qquad (5)$$

$$S_{n+1}^{CH} = \frac{1}{4}S_{zz} + \frac{3}{4}S_{yy} + \frac{\sqrt{3}}{2}S_{yz} \qquad (6)$$

Equations 5 and 6 – Calculation of unsaturated order parameters in united-atom systems using the one-step approach. S_{yy}, S_{zz} and S_{yz} are the *yy*, *zz* and *yz* axes order parameters with respect to the membrane normal, as per Equations 2, 3 and 4. This requires the appropriate definition of the molecular frame of the system, as detailed in the text and shown in Figure 1 (right).

To correctly compute S_{CH} using Equations 5 and 6 requires a different definition of the molecular frame of the system compared to Equations 2, 3 and 4 (Figure 1, right). In particular, the *z* axis is now defined along the C_n-C_{n+1} bond with C_n and C_{n+1} being the carbon atoms within the double bond (e.g. C9 and C10 in the oleoyl tail of POPC), the *x* axis is defined as the normal to the plane defined by C_n and C_{n+1} and the neighbouring methylene carbon atoms C_{n-1} or C_{n+2} (i.e. perpendicular to the predicted C-H bond), while the *y* axis is perpendicular to *x* and *z* axes [44,52,53]. It is worth noting that the terms of Equations 5 and 6 assume 120° for the angles around the double bond. As discussed by Gapsys *et al.* [54], this does not have to be the case and the explicit C_{n-1}-C_n-C_{n+1} and C_n-C_{n+1}-C_{n+2} angles measured from the simulations can be instead used for calculating the terms applied in the S_{CH} calculation. The analysis approach detailed by Equations 5 and 6 is reported as being used in several popular tools, as discussed below. At this point it is also worth noting that while both of the two united-atom analysis approaches have been described as being used in many different publications, the exact tool used to perform the analysis is not always clear and may well be locally written analysis code [1,24,29,55,56].

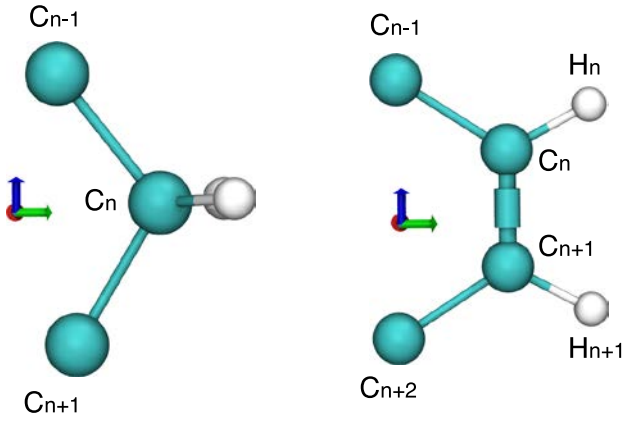

Figure 1 – Pictures showing the atom names referred to in the text and the molecular frames used in the S_{CH} calculations for (left) saturated and (right) unsaturated carbons of the lipid tails. For the axes shown in the pictures, the *z* dimension is in blue, *y* in green and *x* in red.

Simulations and Analysis

To test some of these different methods for calculating lipid tail S_{CH}, we decided to firstly take a previously published all-atom simulation of a POPC membrane [39] generated using the CHARMM36 force field [57], create duplicate trajectories in which we removed the explicit hydrogen atoms to produce a pseudo united-atom CHARMM36 simulation and use both of these to calculate the S_{CH}. In taking such an approach, this allowed us to compare both all-atom and united-atom methods for analysing the same simulation. We note that this is the same approach as described by Pluhackova *et al.* when testing a proposed work-around for known problems within the GROMACS program *g_order* (also termed *gmx order* in recent GROMACS versions) [42]. We also note here that the CHARMM36 force field simulation was first processed with the GROMACS program *trjconv* to ensure none of the lipids were split across the periodic boundary, as some of the tools tested (e.g. the *calc_op.tcl* script and the *g_lomepro* program) produced slightly incorrect results if this were the case (data not shown).

For the all-atom simulation analysis we used: the NMRlipids analysis scripts [41,58,59]; the all-atom script from our previous comparative force field work [39]; the VMD *calc_op.tcl* script [60]; and the Membrainy program [61]. We note here that there are several other tools that could be used to perform such analysis (e.g. [62-65]) which, given the results presented in this work, we expect to produce very similar or identical results for these all-atom systems.

For the pseudo-united-atom simulation, we calculated the S_{CH} using tools that implement one of the two related analysis approaches described above. Tools which use the two-step process were: the united-atom analysis method of the NMRlipids project [41,58,59], a fix to *g_order* provided by Christopher Neale [66,67] (the fix was derived from GROMACS *g_order* version 4.5.4; we note here that there have not been changes to the calculation performed by the standard *g_order*/*gmx order* program in any of the GROMACS versions we checked from 4.5.1 to 2016.2), and the script used in our previous comparative force field work [39]. In the work of the NMRlipids project [68], the GROMACS tool *protonate* is used to explicitly add hydrogen atoms to generate a pseudo all-atom trajectory from a united-atom simulation. This is subsequently followed by the calculation of the S_{CH} using a script implementing Equation 1 [58,59]. In our previous comparative force field work, we wrote a custom script to explicitly calculate the positions of the hydrogen atoms within the lipid tails and used these calculated positions to determine S_{CH} using Equation 1. The results reported in our previous work averaged over hydrogen atoms attached to the same carbon atom. This approach is also taken in a version of the GROMACS program *g_order* provided by Christopher Neale that has a reported fix for calculating S_{CH} of methine (i.e. CH) groups in unsaturated double bonds [66,67]. The original

g_order program, which uses the one-step method, has been reported to incorrectly predict the S_{CH} for such unsaturated double bonds [39,67].

For the one-step united-atom analysis approach, the methods tested were: the original *g_order* tool (GROMACS version 4.5.7); a fix to *g_order* provided by Reid Van Lehn (derived from GROMACS *g_order* version 4.6.2) [53] plus some modifications to this fix described herein; the work-around for the standard *g_order* program of Pluhackova *et al.* (version 4.5.7) [42]; and the *g_lomepro* tool (version 1.0.2) [54]. We note again here that *g_lomepro* does not follow exactly the same approach as Equations 5 and 6, but rather uses a modification of this method which removes the assumption of the ideal 120° angles around the double bond through use of the positions of the carbon atoms in the simulation [54].

Based upon the analysis of the above CHARMM36 simulation, we repeated exactly the same approach using additional all-atom POPC membrane simulations generated with different force fields for several selected analysis tools. These additional simulations were either generated *de novo* or were obtained from the open access data of the NMRlipids project [68,69]. In particular, we performed an additional simulation ourselves using the Slipids force field [70] and obtained an all-atom POPC simulation for the OPLS-AA force field of Maciejewski *et al.* and Kulig *et al.* [71-73] from the NMRlipids project [74]. This further analysis using additional all-atom force fields was performed to ensure that any results obtained were independent of the system and force field used.

The additional Slipids simulation was performed using GROMACS version 5.0.6 [75]. The starting structure was obtained by replicating a CHARMM36 POPC membrane structure, taken from our previous comparative force field study, in *x* and *y* dimensions with the GROMACS program *genconf* to create a membrane containing 512 lipids. Simulations of this membrane were performed for 100 ns using a 2 fs time step, with bonds to hydrogen atoms constrained using the P-LINCS method [76]. The Nosé-Hoover coupling scheme [77,78] and a 2 ps coupling constant was used to maintain the system at a temperature of 298 K. The Parrinello-Rahman pressure coupling scheme [79,80] with a coupling constant of 5 ps was applied to the system in a semi-isotropic manner so as to allow the *x* and *y* box dimensions (within the plane of the membrane) to fluctuate independently of the *z* dimension and to maintain the pressure at an average of 1 bar. Cut-offs were chosen so as to closer replicate those as typically used in AMBER force fields [81], with both Coulombic and van der Waals interactions truncated at 1.0 nm with no long-range dispersion correction applied and PME used to treat the long-range electrostatic interactions [82]. The Verlet cut-off scheme was used [83]. Validation of these cut-off settings with the Slipids force field is provided in the results section. Water was treated using the standard TIP3P model [84].

Once appropriate tools for the analysis of united-atom unsaturated lipid tails had been identified as described in Results and Discussion, we re-analysed some of the simulations performed in our previous comparative force field work [39]. In particular, re-analysis was performed to further examine the splitting of S_{CH} using these united-

atom force fields and to further evaluate the order parameters of the GROMOS 43A1-S3 force field [29]. In addition, we performed further simulations using force fields not studied in this previous work. In particular, we performed POPC membrane simulations of both the OPLS-UA lipids of Ulmschneider *et al.* [85] and the hybrid CHARMM36-UA force field, the latter of which has primarily united-atom lipid tails [33].

For the CHARMM36-UA simulation we used the same membrane starting structure as for the Slipids membrane simulation, with any appropriate hydrogens manually removed and the same general parameters for the simulations applied in this simulation. The only differences were in the cut-off settings that used: the standard CHARMM settings with a Coulombic and van der Waals cut-off of 1.2 nm, force-switching for the van der Waals interactions starting at 1.0 nm, and no long range-dispersion correction [86]. The PME method [82] was used to treat the long-range electrostatic interactions. The CHARMM TIP3P water model was also used [87,88]. As per the Slipids simulation, this CHARMM36-UA simulation was performed using GROMACS version 5.0.6 for 100 ns with a 2 fs time step.

For the OPLS-UA force field POPC simulation, the starting structure containing 128 lipids was initially obtained from the NMRlipids work [89] and extended by 1.2 nm in the *z* dimension to create a slightly bigger system. We note that this starting structure was used as the OPLS-UA POPC structure available from Lipidbook [90] has been reported to have some potential problems with the glycerol backbone structure [91]. The OPLS-UA POPC simulation was performed with GROMACS version 5.1.2 [75] and used: the original TIP3P water model [84], a Coulombic cut-off of 1.0 nm with PME [82] applied for the long-range interactions, and a 1.0 nm cut-off for the van der Waals interactions applied with no dispersion correction for long range van der Waals interactions. All-bonds were constrained using the P-LINCS method [76] allowing a 4 fs time step to be applied in this 500 ns simulation. These settings were chosen to closely match those used by Ulmschneider *et al.* in the original force field parameterization. We note that while a dispersion correction was used in the parameterization of the lipid tails, this was not reported as being applied in the membrane simulations of Ulmschneider *et al.* [85].

Finally, in addition to these new simulations, we also analysed a Berger POPC simulation that used force field parameters for the dihedrals around the double bond of the oleoyl tail that were not studied in our previous work [92,93]. As per the additional OPLS-AA simulation, this simulation was also obtained from open-access data provided by the NMRlipids project [94].

Results and Discussion

Testing of the All-Atom Analysis Tools

We performed the analysis of an all-atom CHARMM36 simulation using several different tools that work on all-atom systems (Figure 2). As can be seen from this

analysis, nearly all of these all-atom analysis tools produce identical results for the analysis of both the *sn*-1 and *sn*-2 chains of the POPC simulation. The only obvious differences that arise between tools are due to the automatic averaging of the S_{CH} for hydrogen atoms attached to the same carbon. This occurs in all of the tools apart from the NMRlipids analysis method, although we note most of the tools tested can be easily modified to report the non-averaged S_{CH}. One important point regarding these results is that the general pattern of a more negative (i.e. smaller) S_{CH} observed for the CHARMM36 force field when compared with the experimental values is exacerbated because this POPC simulation was performed in GROMACS using a potential-switch function for the truncation of the van der Waals interactions rather than a force-based switching function. The latter is now recommended for use with this force field and can be applied in GROMACS [39,86]. Nevertheless, the S_{CH} for carbon 9 in the *sn*-2 oleoyl tail is one area in which improvements could be made for this force field when compared with the experimental data.

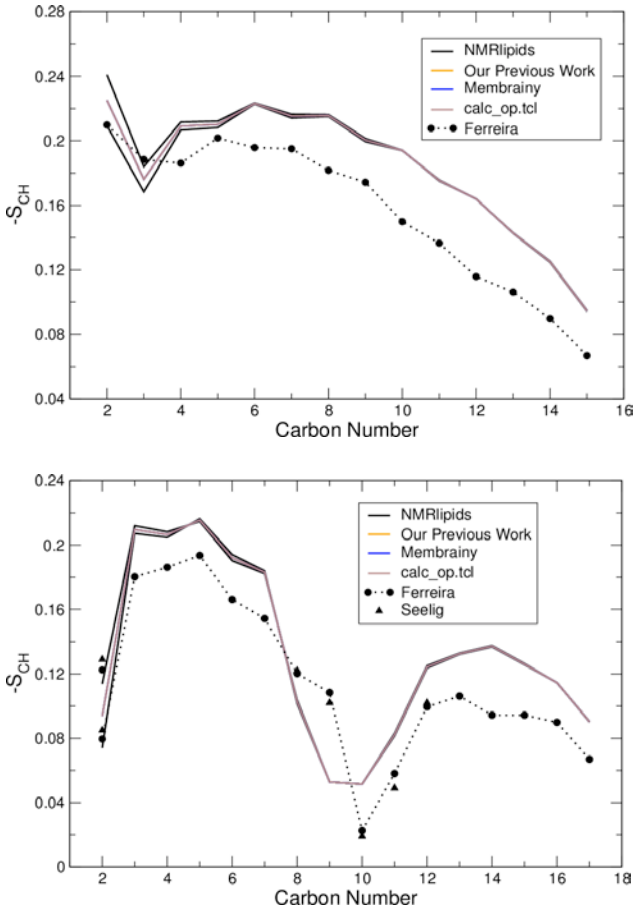

Figure 2 – S_{CH} calculated for the CHARMM36 POPC membrane simulation using all-atom tools. Results are presented for top) the *sn*-1 and bottom) *sn*-2 chains with different tools. As per convention, the figures show $-S_{CH}$. We note that in these two graphs the results from our previous comparative force field study (orange) and the Membrainy program (blue) cannot be seen as they are nearly identical to the results generated with the VMD calc_op.tcl script

(brown). Experimental data from Seelig *et al.* [44] and Ferreira *et al.* [95] are included in the Figure.

Given the agreement of the different all-atom analysis tools we decided to only use one of these tools, the NMRlipids script, to calculate the S_{CH} for the additional two all-atom POPC force field simulations that were studied. These results, presented in Figure 3, provide additional 'gold-standard' results for comparison with the different united-atom analysis tools. We note here that the results presented for all three of these all-atom force fields are in excellent overall agreement with previously published results [57,70,73] and all of the force fields are in good general agreement with the experimentally determined S_{CH}, apart from some of the splitting for carbon 2 of the *sn*-2 chain as discussed below (Figures 2 and 3). One noticeable discrepancy between the results shown in Figure 3 and previously published results arises for the double bond with the OPLS-AA based force field parameters. However, we believe that this occurs from the use of *g_order* in the original work [73]. This is demonstrated in Supporting Figure S1, where we are able to closely reproduce the results reported by Kulig *et al.* using the standard *g_order* approach. As will be discussed in further detail later, the united-atom analysis tool *g_order* does not perform the calculation for the double bond correctly.

In addition to the double bond of the OPLS-AA force field, the other area of the all-atom S_{CH} calculations that show differences to previously reported results are for the splitting of the *pro*-R and *pro*-S S_{CH} of carbon 2 in the *sn*-2 chains. As mentioned in the methods, it has been shown experimentally that these two hydrogen atoms attached to C2 in the *sn*-2 chains of DPPC have non-equivalent order parameters. The absolute value of the S_{CH} for the *pro*-R hydrogen is larger than that of the *pro*-S hydrogen [51]. Given the same size of splitting and temperature dependence of the S_{CH} for these hydrogen atoms in DPPC and POPC [44,96], and similar splitting in lipids with other head group types [97-100], it is reasonable to assume that the smaller absolute value of the S_{CH} for the *pro*-S hydrogen demonstrated for DPPC is also the case in other lipids such as POPC. While the absolute values of these two S_{CH} have been reported in several works [44,95], the sign of the S_{CH} for the *pro*-S hydrogen has been ambiguously reported in the literature. Previously it had been suggested to be positive based upon x-ray membrane structures [45], however NMR experimental work that allows for a measurement of the signs of the S_{CH} demonstrate that both *pro*-R and *pro*-S S_{CH} are almost certainly negative [46,47,101]. Of the three all-atom force fields studied, the CHARMM36 force field is the closest to the experimental data, with an excellent agreement of the splitting of *pro*-S and *pro*-R hydrogen S_{CH} (-0.074 and -0.114 respectively; the experimental values for POPC at 300 K are -0.085/-0.129 [44] and -0.080/-0.123 [95]). These results are also in close agreement with previously reported CHARMM36 simulation results [57,102]. We note the somewhat confusing hydrogen naming in this (and the Slipids) force field, in which the *pro*-R hydrogen is termed atom H2S and the *pro*-S hydrogen atom H2R. While there is also a decent degree of splitting of the *pro*-R and *pro*-S hydrogen S_{CH} in the Slipids simulation, in agreement with the original results reported for POPC [70], there is a qualitative disagreement with the experimental results. This is because the *pro*-S hydrogen atom S_{CH} is substantially

smaller than that of the *pro*-R hydrogen atom S_{CH} (-0.145 and -0.100 respectively; Figure 3). We note that this was not reported in the original publication of the POPC parameters with this force field and is an area in which future improvements could, therefore, be made. Finally, there is less splitting of the two order parameters with the OPLS-AA force field parameters and smaller S_{CH} values for both hydrogen atoms. However, unlike with the Slipids force field, the *pro*-S hydrogen S_{CH} is larger than the *pro*-R value (-0.147 and -0.172 respectively). This is also, therefore, an area of future improvement for these force field parameters.

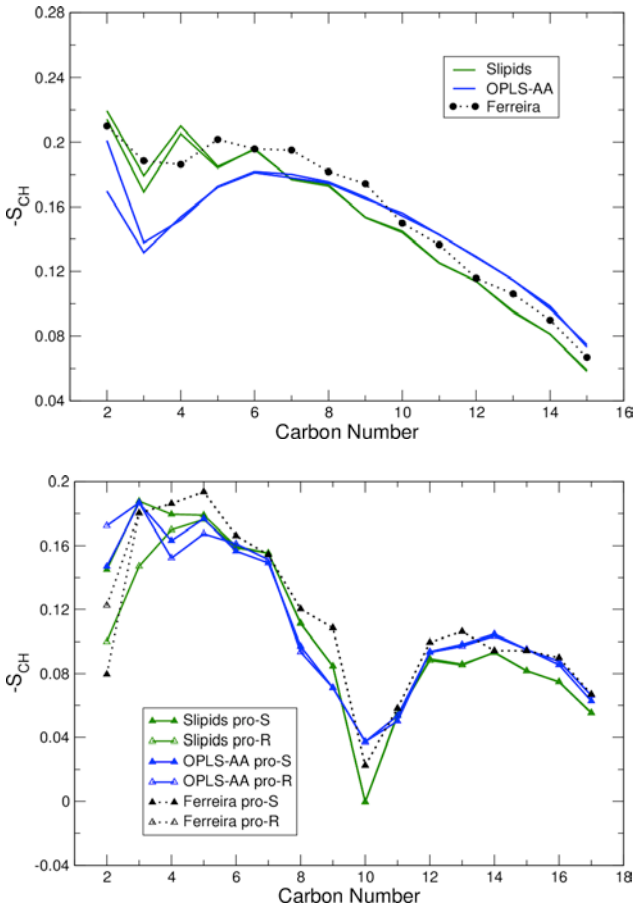

Figure 3 – S_{CH} calculated for the Slipids and OPLS-AA POPC simulations using the NMRlipids analysis tool. Results are presented for top) the *sn*-1 and bottom) *sn*-2 chains and are separated for the *pro*-R and *pro*-S hydrogen atoms to demonstrate any splitting of the S_{CH}. Experimental data from Ferreira *et al.* [95] is also included in the Figure.

We also examined several other properties of the Slipids POPC membrane because this simulation was performed using substantially different cut-off settings to the original force field publication, so as to closer match the cut-off scheme used in AMBER force fields. The membrane properties, shown in Figure S2, are in good agreement with the corresponding range of experimentally determined values. Hence, this cut-off scheme is appropriate for use with this lipid force field in, for example, the context of a membrane-protein simulation with the AMBER99SB-ILDN force field [81].

We note that using this 1.0 nm cut-off also substantially improves performance when using the Verlet cut-off scheme in GROMACS.

Testing of the United-Atom Analysis Tools

Saturated Palmitoyl Chain – All Force Fields

Having obtained consistent reference all-atom results, we began to analyse the united-atom analysis tools, firstly using the pseudo united-atom CHARMM36 POPC simulation. The results in Figure 4 show that all the analysis methods produce very similar results for the *sn*-1 palmitoyl tail, albeit with S_{CH} for the individual hydrogen atoms averaged in all of the methods except for the NMRlipids united-atom approach. In addition to the results presented in Figure 4, we have made further additions to the version of *g_order* provided by Reid Van Lehn [53], implementing Equations 3 and 4 to calculate the S_{CH} of the individual hydrogen atoms in the united-atom methylene groups. The results from this modified version of *g_order* are nearly identical results to the NMRlipid united-atom approach (Figure S4). All of these results are also in close agreement with the reference all-atom results. Analysis of the additional all-atom POPC simulations with different force fields using the standard GROMACS *g_order* program, demonstrates that this close agreement to the all-atom results for the *sn*-1 chain is generally maintained across different membrane structures and force fields (Figure 4). We note that there are some slightly larger discrepancies with the OPLS-AA force field in particular, that will be addressed in further detail when discussing the oleoyl chain results.

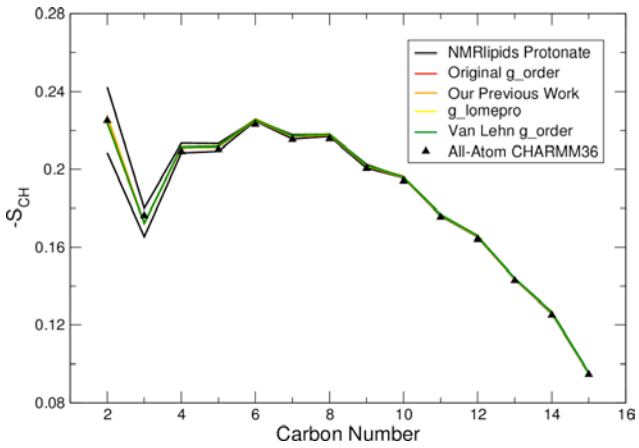

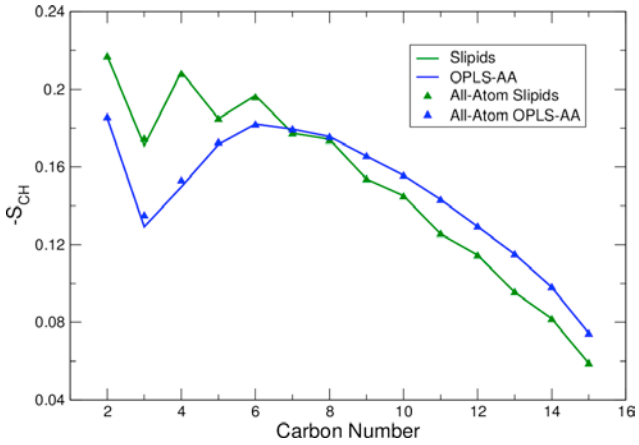

Figure 4 – S_{CH} calculated for the *sn*-1 tail of the CHARMM36 POPC simulation using the different united-atom analysis methods (top) and for the Slipids and OPLS-AA POPC simulation *sn*-1 chain using the standard *g_order* program (bottom). The averaged results calculated using the NMRlipids all-atom analysis method are also shown for reference. We note that analysis methods that do not alter the calculation performed by the standard *g_order* program for the saturated carbons (Neale and Pluhackova methods) are not shown in the top figure for clarity.

Unsaturated Oleoyl Chain – CHARMM36 Parameters

For the *sn*-2 oleoyl tail, which contains a double bond between carbon atoms 9 and 10, there are, however, deviations in the calculated S_{CH} between the different methods and the CHARMM36 reference results (Figure 5). As in the *sn*-1 tail, the majority of the S_{CH} of the methylene carbons are very similar between all the different methods used. However, around the double bond (i.e. carbon atoms 8-11), substantial deviations between the methods arise.

First, the S_{CH} calculated using the two-step analysis process (i.e. the NMRlipids script, the modified version of *g_order* provided by Christopher Neale, and the script used in our previous comparative force field work) do not result in the same S_{CH} as either the all-atom results or with each other (Figure 5). Given the relative simplicity of the calculation of the S_{CH} using Equation 1, and the fact that both the NMRlipids tool and the script used in our previous comparative force field work provide the same (and correct) order parameters for the all-atom system (Figure 2) demonstrates that the differences arise in the addition of the hydrogen atoms. While the *protonate* approach used in the NMRlipids united-atom analysis method does give results in closer agreement with the all-atom reference results, both of the other two tools demonstrate substantial deviation for C9 and C10. Further examination of the (same) method used in the modification by Christopher Neale to *g_order* and within the united-atom analysis script from our previous comparative force field work identified that these approaches add the methine hydrogen atom incorrectly, retaining a close to tetrahedral geometry. This is highlighted in Figure S3, where S_{CH} generated using these two methods and S_{CH} generated using the standard *g_order* program without the '*–unsat*' option for C9 and C10, produce nearly identical results. As for the

differences between the all-atom and united-atom results produced by the NMRlipids analysis, this arises because the CHARMM36 all-atom force field does not simply use idealised geometries for the positions of methine hydrogen atoms (H_n and H_{n+1}) based upon vectors bisecting the C_{n-1}-C_n-C_{n+1} and C_n-C_{n+1}-C_{n+2} angles as the analysis method assumes (see Figure 1 for the naming conventions). Rather, given the fact that the hydrogen atoms are explicit, their positions can be further modified by additional parameters within the force field and interactions formed during the simulations. For example, the C_{n-1}-C_n-H_n and H_{n+1}-C_{n+1}-C_{n+2} angles are defined as 116° in the CHARMM36 force field. This all leads to an actual positioning of the H_n and H_{n+1} atoms in the simulation that are not respectively bisecting the C_{n-1}-C_n-C_{n+1} and C_n-C_{n+1}-C_{n+2} angles of the double bond.

In addition, disagreements between the CHARMM36 all-atom reference results also arise using some of the united-atom analysis tools that report to follow the one-step calculation approach (Figure 5 and Figure S5). The incorrect calculation using the standard GROMACS tool *g_order* is not surprising given that this has been reported before and is a known problem within this tool that is still present in the most recent versions of GROMACS [67]. In addition, an initial version of another fix to the *g_order* tool provided by Reid Van Lehn [53] also produced an incorrect order parameter for C10 (i.e. the second carbon of the double bond, C_{n+1}) (Figure S5). However, including minor modifications made to correct the calculation performed by this tool for these unsaturated carbon atoms (see the legend of Figure S5 for more details) results in S_{CH} now in much closer agreement with the all-atom results (Figure 5). We note that we have also made further additions to this modified version of *g_order* to calculate the individual hydrogen atom S_{CH} in the methylene groups, as discussed above (Figure S4). This does, however, raise the question of why this relatively close agreement occurs, given that CHARMM36 (and indeed every one of the all-atom force fields studied in this work) does not use 120° for the C_{n-1}-C_n-C_{n+1} and C_n-C_{n+1}-C_{n+2} angles of the double bond yet this one-step analysis method inherently assumes ideal 120° angles around the methine groups. This can, however, also be explained by the point raised previously regarding the NMRlipids united-atom analysis: the all-atom force fields modify the positions of the hydrogen atoms through additional force field parameters and interactions. This modification of the hydrogen atom positions in the all-atom system results in C_{n+1}-C_n-H_n and C_n-C_{n+1}-H_{n+1} angles that are now slightly closer to 120° (as inherently assumed in the one-step calculation) compared with if the hydrogen atoms are positioned along the vectors bisecting the C_{n-1}-C_n-C_{n+1} and C_n-C_{n+1}-C_{n+2} angles (as is done in the two-step NMRlipids united-atom approach).

To explore this further and to try and perform a united-atom analysis that closer matches the all-atom results, we calculated all the time-averaged angles around the double bond in the CHARMM36 all-atom simulation using the GROMACS program *g_angle*. Taking the average of the calculated C_{n+1}-C_n-H_n and C_n-C_{n+1}-H_{n+1} angles (118.3°), we manually implemented the S_{CH} calculation of Seelig *et al.* [44] (using this averaged angle to calculate θ as defined in Appendix A of the work of Seelig *et al.*) as an option within our modifications to the fixed version of the *g_order* tool. This

manual implementation modifies the terms of Equations 5 and 6 to use this angle measured from the original all-atom simulation, instead of 120°. The results for this manual implementation are also shown in Figure 5. These results demonstrate that, as expected, using the average value of the actual positions of the hydrogen atoms within this united-atom analysis approach, results in the closest agreement with the all-atom reference results. This also further demonstrates the correct working of our fix to the Reid Van Lehn modified *g_order* program in implementing the approach of Equations 5 and 6.

As described in the methods, we also tested the work around to the standard *g_order* program proposed by Pluhackova *et al.* and in agreement with the results reported in that work, this method does produce S_{CH} in close agreement with the CHARMM36 reference results (Figure 5). However, as will be shown below, we believe this only arises for this force field due to a cancellation of errors and is not applicable across all force fields.

Finally, it can be seen that the *g_lomepro* program also produces identical S_{CH} for the unsaturated carbons as the NMRlipids tool, which is not surprising given that both methods use the measured C_{n-1}-C_n-C_{n+1} and C_n-C_{n+1}-C_{n+2} angles during their S_{CH} calculation approaches (Figure 5). It is important to note here, however, that to get *g_lomepro* to perform an accurate calculation on the POPC *sn*-2 oleoyl tail required use of either the '*–unsat 2*' option of the program or use of the '*–unsat 1*' option with subsequent selection of the appropriate *sn*-2 lipids groups (for the tail and the unsaturated groups) as the prompted *sn*-1 option. Not taking either of these approaches resulted in the same order parameters for the double bond carbons as those produced when they were treated as fully saturated by the *g_lomepro* program (i.e. close to the results shown in Figure S3).

As an additional further test of our modifications to the *g_order* program, a manual implementation of the angle α, as defined by Gapsys *et al.* [54], using the CHARMM36 C_{n-1}-C_n-C_{n+1} and C_n-C_{n+1}-C_{n+2} average simulation angles (126.6°) within the corrected version of *g_order* was also able to reproduce the *g_lomepro* and NMRlipids united-atom results (Figure S6). This again demonstrates that this fixed version of *g_order* works correctly.

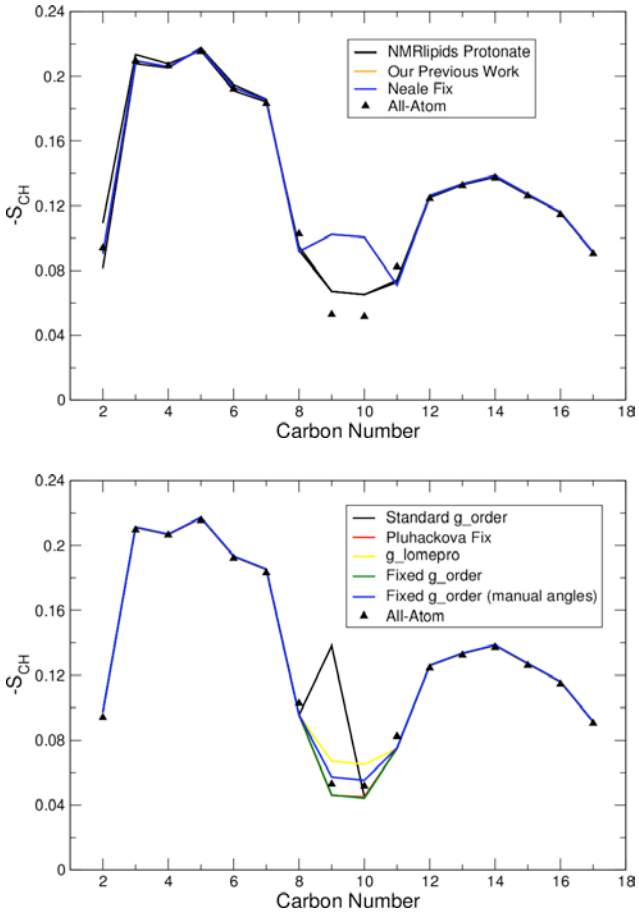

Figure 5 – S_{CH} calculated for the *sn*-2 tail of the CHARMM36 POPC simulation using the different united-atom analysis methods. Results for tools that use the two-step analysis approach are shown in the top graph, while results for tools using the one-step approach are shown in the bottom graph. The averaged results calculated using the NMRlipids all-atom analysis method are also shown for reference. We note that in the top graph, the results from our previous comparative work cannot be seen as they are identical to those produced by Christopher Neale's modified version of *g_order* (see Figure S3 for a clear demonstration of this). For the fixed version of *g_order* (bottom graph), the methylene S_{CH} shown are of the averages of the two hydrogen atoms.

Unsaturated Oleoyl Chain – Slipids and OPLS-AA Parameters

Given the results presented in Figure 5, we chose to only use the united-atom analysis tools that produced S_{CH} in a fairly close agreement with the all-atom CHARMM36 reference results for analysis of the two other pseudo united-atom (i.e. derived from all-atom) POPC force field simulations (Figure 6). These tools were the NMRlipids united-atom script, our modifications to the version of *g_order* provided by Reid Van Lehn and the work-around for the standard *g_order* program of Pluhackova *et al.* We note that while the *g_lomepro* tool also produced results in fairly close agreement with the all-atom reference simulation, it was not studied further as it produces identical results to the NMRlipids united-atom script apart from the automatic

averaging of *pro*-R and *pro*-S hydrogen atoms attached to the same carbon atom. All further discussion regarding the results of the unsaturated carbon S_{CH} with the NMRlipids united-atom analysis tool can equally be applied to results produced with the *g_lomepro* program.

Figure 6 shows that the approach of Pluhackova *et al.* does not agree with the all-atom reference data when applied to the other all-atom force fields studied. In all cases, the NMRlipids united-atom tool slightly overestimates the S_{CH} of the carbons in the double bond, while the fixed version of *g_order* implementing the approach of Equations 5 and 6 slightly underestimates the ordering of these carbons. It is also worth noting here that the analysis performed using the modified version of *g_order* is substantially faster to perform than using the NMRlipids united-atom tool. In addition to testing these three methods, we also tested the manual implementation of the CHARMM36 C_{n+1}-C_n-H_n and C_n-C_{n+1}-H_{n+1} averaged angles in our modified version of *g_order*. We deemed this implementation appropriate to test as the same calculated angles in the other all-atom force fields were both in close agreement with the CHARMM36 value of 118.3° (Slipids: 118.3° and OPLS-AA: 117.7°). Given the close agreement of this angle in the all-atom force field simulations, this analysis method once again results in the closest agreement with the all-atom reference results (Figure 6).

It is also worth noting that the results for the OPLS-AA force field parameters also show slight discrepancies between the all-atom results and the united-atom methods for some of the saturated carbons near the glycerol region of the lipid, with all the united-atom methods reproducing one another. These differences presumably arise due to deviation from ideal tetrahedral geometry in these methylene groups. We note that this simulation was both the shortest trajectory analysed in this work and also contained the fewest simulation frames, given that it was downloaded from the NMRlipids project. We suspect, therefore, that this result may have arisen either due to a lack of sampling or could be an issue with the force field itself used in this simulation.

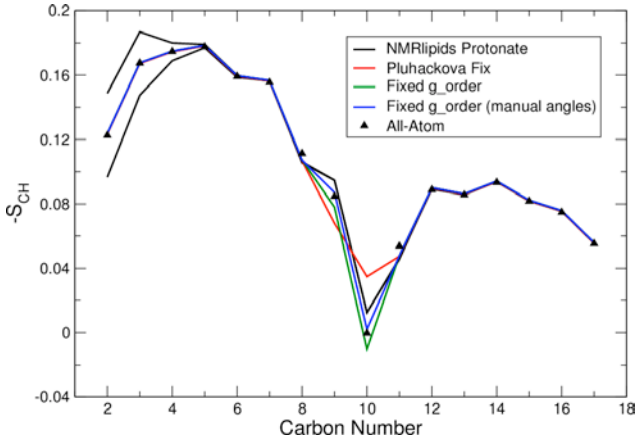

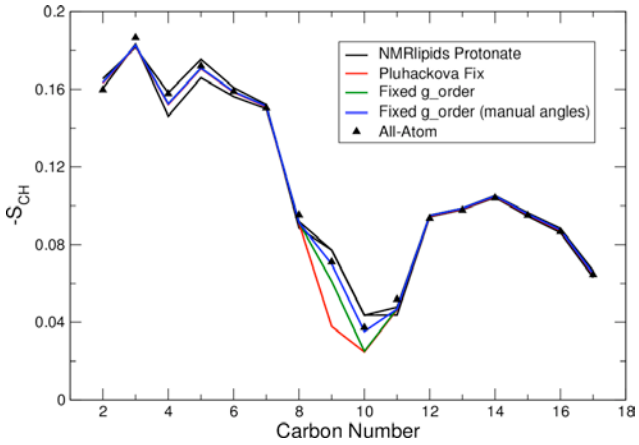

Figure 6 – S_{CH} calculated for the *sn*-2 tail of the Slipids (top) and OPLS-AA (bottom) simulations using the different united-atom analysis methods. The averaged results calculated using the NMRlipids all-atom analysis method are also shown for reference. The method proposed by Pluhackova *et al.* (red) does not produce S_{CH} close to the all-atom results for these two force fields, while the implementation of the manual hydrogen angles into the fixed version of *g_order* produces the closest match to the all-atom results. As with the CHARMM36 analysis, the results shown with our modified fixed version of *g_order* are the averages of the two hydrogen atoms in methylene groups.

Overall, these results highlight that, in their current state, the majority of the tested united-atom tools should not be used in the calculation of S_{CH} for carbons within the double bound of unsaturated united-atom lipid tails. Indeed, based upon the comparisons to all-atom simulations, of all of the tools tested herein, we would only recommend the use of the modified version of *g_order* primarily constructed by Reid Van Lehn and further modified and added to herein (provided within the Supporting Information of this work), the NMRlipids united-atom analysis scripts, or the *g_lomepro* tool (when used as described above). Additionally, this recommendation is only for united-atom force fields in which the C_{n-1}-C_n-C_{n+1} and C_n-C_{n+1}-C_{n+2} angles are 120°. For united-atom force fields where this is not the case, the situation is slightly more complicated and will be discussed in further detail below.

Calculation of Order Parameters from United-Atom Simulations

Revisiting Previously Reported Order Parameters

Given the aforementioned problems in the calculation of S_{CH} for the double bond of united-atom POPC lipids we decided to re-calculate the S_{CH} from the united-atom POPC simulations within the “Simulations with Optimal Parameters” section of our previous comparative force field work [39] using the newly validated *g_order* program. Indeed, the averaged results generated from the final 100 ns of these simulations using the fixed version of *g_order* have recently been published within a correction to that work [49]. However, to put these findings in the context of the current study, we will briefly discuss the results here.

For all four united-atom force fields studied previously, there are differences observed for the C9 and C10 order parameters. While most of the S_{CH} are still somewhat similar to those originally reported, there are larger differences observed for the GROMOS 43A1-S3 force field [29]. We note here, that this force field does not use 120° angles around the double bond and so this analysis must be considered carefully, as will be discussed below. Through a comparison with the experimentally determined S_{CH}, these new results for the GROMOS 43A1-S3 force field now reverse one of the recommendations made from this previous work. In particular, we would now recommend the use of this force field for POPC simulations, despite some disagreement with the S_{CH} both in and after the double bond. We also wish to apologise for these previously incorrectly drawn conclusions, especially given the publication of very similar results to our corrected S_{CH} using this force field [55,103].

In addition to this published correction of the reported S_{CH}, we also sought to further examine the order parameters from these united-atom simulations. In particular, by employing the analysis methods used in both the NMRlipids project and in our additions to the fixed version of *g_order*, it is possible to separate the order parameters for the individual hydrogen atoms in the methylene groups (Figure 7). Therefore, we are now able to explicitly determine whether the united-atom force fields can reproduce the experimentally observed differences of the order parameters for the second carbon in the *sn*-2 chain. As far as we are aware this splitting of the S_{CH} at carbon atom 2 has not been extensively studied in united-atom systems. We note here that, as for the CHARMM36 analysis (Figure S4), these two different analysis methods generally produce very similar results for the individual hydrogen atom S_{CH} albeit with some slight differences arising for C2 (Figure 7). For C2, the NMRlipids analysis method produces a closer match to the CHARMM36 all-atom reference results (Figure 2 and S4), with a slightly larger splitting between the *pro*-R and *pro*-S hydrogen atoms than that calculated with the fixed version of *g_order*.

The results presented in Figure 7 demonstrate a notable degree of splitting of the C2 S_{CH} for the *sn*-2 chain in the GROMOS 43A1-S3 and GROMOS-CKP simulations, despite the united-atom nature of these force fields. For GROMOS 43A1-S3, this splitting is not in qualitative agreement with the experimentally determined values as the S_{CH} for the *pro*-S hydrogen atom is smaller than that of the *pro*-R hydrogen atom (-0.202 and -0.122 respectively using the NMRlipids analysis method and -0.203 and -0.121 using the fixed version of *g_order*) [44,95,100]. For the GROMOS-CKP parameters, the results are in reasonable agreement with the experimentally derived values despite more overall ordering; the S_{CH} for the *pro*-S and *pro*-R hydrogen atoms are -0.123 and -0.180 respectively with the NMRlipids method and -0.128 and -0.173 with the fixed version of *g_order*. We note here, however, that the amount of S_{CH} splitting at C2 with this force field is somewhat variable between repeat simulations and these reported values are the largest splitting observed from several different simulations (Table S1). While there is relatively little splitting of the C2 S_{CH} in the Berger and GROMOS $53A6_L$/54A7 force fields shown in Figure 7, in both cases the S_{CH} for the *pro*-S hydrogen atom is larger than that of the *pro*-R hydrogen atom (-

0.153 and -0.163; -0.144 and -0.158; respectively for the Berger and GROMOS $53A6_L$/54A7 force fields with the NMRlipids method). The lack of substantial S_{CH} splitting in the Berger force field is in agreement with previously reported results [93]. As with the GROMOS-CKP force field, the amount of S_{CH} splitting at C2 with the GROMOS $53A6_L$ force field is variable across repeat simulations and can result in greater splitting of these order parameters than shown in Figure 7 (Table S2). However, this is not on average to the same degree as in the GROMOS-CKP simulations; the mean differences in the *sn*-2 tail C2 *pro*-R and *pro*-S S_{CH} from six simulations of the GROMOS-CKP and GROMOS $53A6_L$ force fields are 0.039 and 0.022 respectively (Tables S1 and S2, NMRlipids analysis method). This difference between the GROMOS-CKP and GROMOS $53A6_L$ force fields is interesting given their similarity; the only differences in the glycerol and tail parts of the lipid are the larger van der Waals radii of the carbonyl carbons (C1) in the GROMOS-CKP parameters. We assume that the increased van der Waals radii in the GROMOS-CKP simulation are having a serendipitous effect upon the orientation of C2 and inducing a larger splitting of the S_{CH}, at least over the 200 ns timescales of these simulations. We stress again here that the amount of splitting at C2 in the *sn*-2 chain is variable across GROMOS-CKP and GROMOS $53A6_L$ simulations, irrespective of starting structure used (Tables S1 and S2). We suspect that this may be due to long-lived metastable states within this region for these two closely related force fields. From analysis of other simulations in our previous comparative force field work, the Berger and GROMOS 43A1-S3 force fields do not have this issue (data not shown).

Re-analysis of these four united-atom POPC force field simulations using the NMRlipids scripts also demonstrates that the GROMACS *protonate* approach produces nearly identical results for three of the four force fields when compared to the same results produced with the corrected version of *g_order* (Figure 7). This re-iterates our conclusions drawn above, namely we recommend both of these tools for united-atom force fields that use 120° C_{n-1}-C_n-C_{n+1} and C_n-C_{n+1}-C_{n+2} angles for the double bond. The averaged values of these angles, calculated from the simulations, are 119.8°, 120.5° and 120.5° for the Berger, GROMOS$53A6_L$ and GROMOS-CKP force fields respectively. The GROMOS 43A1-S3 force field is the only force field in which the results between the two methods substantially differ because it does not use these 120° bond angles. Indeed, the combined average of the calculated angles from the GROMOS 43A1-S3 simulation is 128.2°. As discussed above, the S_{CH} of the all-atom systems are typically in between the results generated using the corrected version of *g_order* and the NMRlipids united-atom scripts. In the all-atom simulations the hydrogen atom positions can be modified from idealised geometries, resulting in a geometry used for the S_{CH} calculation in which the actual C_{n+1}-C_n-H_n and C_n-C_{n+1}-H_{n+1} angles from the simulation are in between those predicted using the measured C_{n-1}-C_n-C_{n+1}/C_n-C_{n+1}-C_{n+2} angles and 120° angles. Therefore united-atom force fields in which the C_{n-1}-C_n-C_{n+1} and C_n-C_{n+1}-C_{n+2} angles deviate from 120° are likely to have the most appropriate S_{CH} somewhere in between those produced by these two analysis methods, based upon the results of the three all-atom force fields studied in this work. Despite this, however, we believe that using a completely idealised 120° geometry for

the double bond S_{CH} calculation with GROMOS 43A1-S3 force field produces a reasonably realistic representation of these S_{CH} with this force field. This method was also used in the original S_{CH} POPC calculation with this force field [55], and it is for these two reasons why the fixed version of *g_order* was used for the corrections reported to our previous comparative force field work with the GROMOS 43A1-S3 force field [49]. Furthermore, if we compare the results presented for this force field in Figure 7, the same recommendations as made in the correction to our previous comparative force field work hold true even when looking at the other extreme of predicted values of the GROMOS 43A1-S3 double bond S_{CH} as produced by the NMRlipids united-atom analysis method.

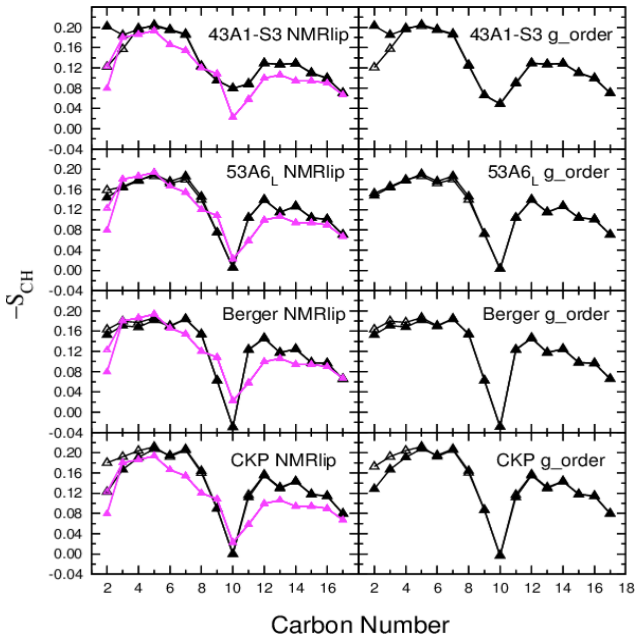

Figure 7 – S_{CH} calculated for the *sn*-2 tail of the four united-atom POPC force field simulations using both the NMRlipids united-atom analysis method (graphs on the left), and the fixed version of *g_order* validated above (graphs on the right). The results are shown explicitly for both *pro*-R (open triangles) and *pro*-S (filled triangles) hydrogen atoms. We note that the results obtained from the fixed version of *g_order* are almost identical to those we recently reported in the correction to our previous work [49]. The only differences result from the analysis here being performed on the complete 200 ns simulations and the individual hydrogen atom results being reported. Experimental data from Ferreira *et al.* [95] is also included in the NMRlipids graphs (magenta) for reference.

Analysis of Additional United-Atom Force Fields

We also sought to examine order parameters of united-atom POPC force fields not simulated in our previous comparative force field work. Specifically, we performed or obtained POPC simulations using the Berger force field with modified dihedrals applied around the double bond, the CHARMM36-UA force field and the OPLS-UA

force field. The results for these force fields are presented in Figure 8, using both the NMRlipids and fixed *g_order* analysis methods.

In agreement with the results already presented, the differences between these two methods for the carbon atoms in the double bonds increases as the C_{n-1}-C_n-C_{n+1} and C_n-C_{n+1}-C_{n+2} angles deviate further from 120° (Berger with the Bachar dihedrals: 122.6°; CHARMM36-UA: 124.1°; OPLS-UA: 125.7°). In agreement with previously published results, the implementation of the Bachar *et al.* dihedrals [92], originally designed for polyunsaturated lipid tails, improves the agreement with the experimental S_{CH} for the Berger force field at the double bond [93]. For the CHARMM36-UA force field there is also good agreement with the previously reported S_{CH}. For the double bond, where there is some deviation between the two analysis methods, the S_{CH} calculated with the fixed version of *g_order* is in close agreement with the original published results. There is also a good degree of splitting of the S_{CH} at carbon 2 (-0.079 and -0.108 for the *pro*-S and *pro*-R hydrogen atoms respectively), which is not surprising given the explicit inclusion of the hydrogen atoms for this carbon within this hybrid force field [33]. For the OPLS-UA force field, we are not aware of any previously reported S_{CH} for the double bond. The S_{CH} are in reasonable agreement with the experimental values for this region of the *sn*-2 tail, albeit with more substantial deviations depending upon which analysis method is used. We stress again here that we believe the most appropriate S_{CH} for the carbon atoms in the double bond would likely lie in between the two values reported, given the analysis of the three different all-atom systems. The most substantial disagreement with the experimental order parameters for this OPLS-UA force field arises in the splitting of the S_{CH} at carbon 2. As with the Slipids force fields, the S_{CH} of the *pro*-S hydrogen is smaller than that of the *pro*-R hydrogen (-0.136 and -0.063 respectively).

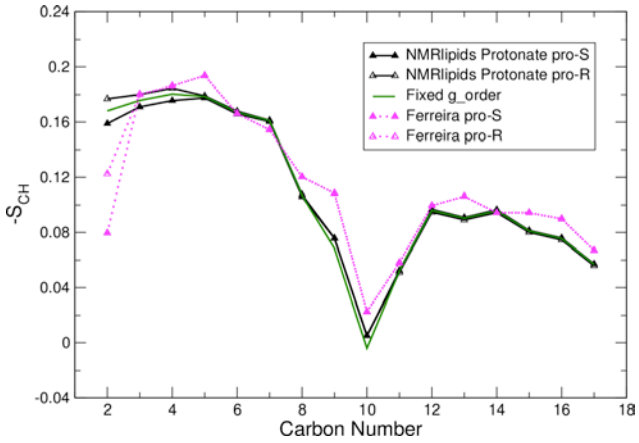

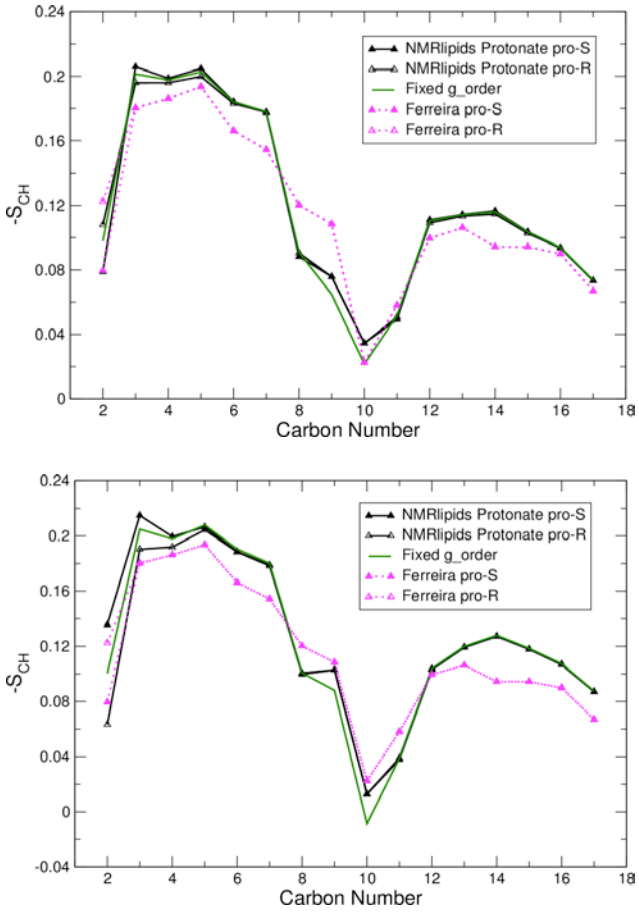

Figure 8 – S_{CH} calculated for the *sn*-2 tail of the additional three united-atom POPC force fields not studied in our previous comparative work. The Berger force field with the Bachar parameters for the double bond is shown in the top graph, the CHARMM36-UA force field in the middle and the OPLS-UA force field in the bottom graph. S_{CH} were calculated using both the NMRlipids united-atom analysis method (black lines) and the fixed version of *g_order* validated above (green lines). The results obtained using the NMRlipids method are shown explicitly for both *pro*-R (open triangles) and *pro*-S (filled triangles) hydrogen atoms to demonstrate any splitting of the S_{CH} while the results generated using the fixed version of the *g_order* program show the averages. Experimental data from Ferreira *et al.* [95] is also included in the graphs.

Conclusions

A re-evaluation of several common tools used to calculate the carbon-hydrogen order parameters of lipid tails from united-atom simulations has revealed that most of the current tools used for analyzing unsaturated lipid tails produce incorrect results. Consequently, we suggest that most simulation papers reporting united-atom order parameters for unsaturated lipids will likely contain errors to a greater or lesser extent. The degree of error will depend upon both the force field and the analysis tool used. Only publications where the analysis was performed with locally written tools, the NMRlipids united-atom approach, or the *g_lomepro* program (as used here) will have

obtained accurate results (although, as we have discussed, for some united-atom force fields such as GROMOS 43A1-S3 it is difficult to say what the best predicted order parameters are).

We also used validated tools to assess the splitting of the *sn*-2 chain carbon 2 in both all-atom and united-atom POPC membrane systems. In agreement with previously reported results, the CHARMM36 and CHARMM36-UA force fields closely reproduced the experimental splitting for the two hydrogen atoms attached to this carbon atom. In addition, we also observed the most appropriate splitting of the *pro*-R and *pro*-S S_{CH} in the GROMOS-CKP force field, which we believe arises fortuitously due to the larger size of the carbonyl carbon's van der Waals radius within this force field. However, the amount of splitting is variable across simulations with this force field. Interestingly, the splitting observed with the Slipids force fields results in S_{CH} in disagreement with experimental values as the *pro*-R S_{CH} is larger than that of the *pro*-S hydrogen atom. Indeed, this is also true for the united-atom GROMOS 43A1-S3 and OPLS-UA force fields. With relatively little splitting of the S_{CH} observed in the OPLS-AA, Berger and GROMOS 53A6$_L$ force fields, this property is an area that needs further attention in most of the current lipid force fields.

Despite further planned modifications to improve the fixed version of the *g_order* program (e.g. so as to use the positions of hydrogen atoms when present in an all-atom simulation and to allow use the actual simulation C_{n-1}-C_n-C_{n+1} and C_n-C_{n+1}-C_{n+2} angles for the S_{CH} calculation), the tool in its current state is provided in the Supporting Information of this work. In addition, some basic documentation (Appendix S1) and example input files for the united-atom force fields studied herein are also provided. This will immediately allow the rapid and accurate calculation of order parameters from united-atom simulations in which double bonds are present within the lipid tails, and also enable quick and accurate determination of splitting or forking of hydrogen atom S_{CH} in united-atom methylene groups.

Author Information

Author Contributions

Conceived, designed and performed the work: TJP
Contributed ideas, materials and resources: JRA, RBS and JWE
Wrote the manuscript: TJP
Made manuscript improvements: JRA, RBS and JWE

The authors declare no competing financial interests.

Supporting Information

The supporting information consists of: a document containing six additional figures; two tables; an appendix detailing installation and usage instructions for the fixed version of *g_order*; six input text 'dat' files for running the fixed version of *g_order*

with the different united-atom force fields studied in this work; and source code of the fixed version of *g_order*. This information is available free of charge via the Internet at http://pubs.acs.org.

Acknowledgements

We thank Ángel Piñeiro for his invaluable help particularly with the analysis tool from our previous work, Ivan Welsh for double-checking the C2 prochirality and Reid Van Lehn for the provision of his modified version of *g_order*. TJP wishes to thank Jonathan David and Jamie Taylor at Dstl for their continued support, and Iain and the late Janette Piggot for providing the computational resources utilized in majority of this work. This work was supported financially by Dstl. We wish to acknowledge use of the Iridis Computational Facilities at the University of Southampton and the BlueCrystal Computational Facilities at the University of Bristol. Finally, we wish to acknowledge the excellent work of the NMRlipids project, whose on-going work and open access analysis methods were one of the key driving forces behind this study.

References

(1) Heller, H.; Schaefer, M.; Schulten, K., Molecular Dynamics Simulation of a Bilayer of 200 Lipids in the Gel and in the Liquid Crystal Phase. *J. Phys. Chem-US* **1993**, *97* (31), 8343-8360.

(2) Marrink, S.; Lindahl, E.; Edholm, O.; Mark, A., Simulation of the Spontaneous Aggregation of Phospholipids into Bilayers. *J. Am. Chem. Soc.* **2001**, *123* (35), 8638-8639.

(3) Tieleman, D. P.; Berendsen, H. J. C.; Sansom, M. S. P., An Alamethicin Channel in a Lipid Bilayer: Molecular Dynamics Simulations. *Biophys. J.* **1999**, *76* (4), 1757-1769.

(4) Tieleman, D. P.; Leontiadou, H.; Mark, A. E.; Marrink, S.-J., Simulation of Pore Formation in Lipid Bilayers by Mechanical Stress and Electric Fields. *J. Am. Chem. Soc.* **2003**, *125* (21), 6382-6383.

(5) Marrink, S.-J.; Mark, A. E., Molecular View of Hexagonal Phase Formation in Phospholipid Membranes. *Biophys. J.* **2004**, *87* (6), 3894-3900.

(6) Falck, E.; Róg, T.; Karttunen, M.; Vattulainen, I., Lateral Diffusion in Lipid Membranes through Collective Flows. *J. Am. Chem. Soc.* **2008**, *130* (1), 44-45.

(7) Piggot, T. J.; Holdbrook, D. A.; Khalid, S., Electroporation of the *E. coli* and *S. aureus* Membranes: Molecular Dynamics Simulations of Complex Bacterial Membranes. *J. Phys. Chem. B* **2011**, *115* (45), 13381-13388.

(8) Nagai, T.; Okamoto, Y., Replica-Exchange Molecular Dynamics Simulation of a Lipid Bilayer System with a Coarse-Grained Model. *Mol. Simulat.* **2012**, *38* (5), 437-441.

(9) Koldsø, H.; Shorthouse, D.; Hélie, J.; Sansom, M. S. P., Lipid Clustering Correlates with Membrane Curvature as Revealed by Molecular Simulations of Complex Lipid Bilayers. *PLoS Comput. Biol.* **2014**, *10* (10), e1003911.

(10) Lyubartsev, A. P.; Rabinovich, A. L., Force Field Development for Lipid Membrane Simulations. *BBA - Biomembranes* **2016**, *1858* (10), 2483-2497.

(11) Neale, C.; Bennett, W. F. D.; Tieleman, D. P.; Pomès, R., Statistical Convergence of Equilibrium Properties in Simulations of Molecular Solutes Embedded in Lipid Bilayers. *J. Chem. Theory Comput.* **2011**, *7* (12), 4175-4188.

(12) Mori, T.; Miyashita, N.; Im, W.; Feig, M.; Sugita, Y., Molecular Dynamics Simulations of Biological Membranes and Membrane Proteins Using Enhanced Conformational Sampling Algorithms. *BBA - Biomembranes* **2016**, *1858* (7, Part B), 1635-1651.

(13) Klauda, J. B.; Brooks, B. R.; Pastor, R. W., Dynamical Motions of Lipids and a Finite Size Effect in Simulations of Bilayers. *J. Chem. Phys.* **2006**, *125* (14), 144710.

(14) Chowdhary, J.; Harder, E.; Lopes, P. E. M.; Huang, L.; MacKerell, A. D.; Roux, B., A Polarizable Force Field of Dipalmitoylphosphatidylcholine Based on the Classical Drude Model for Molecular Dynamics Simulations of Lipids. *J. Phys. Chem. B* **2013**, *117* (31), 9142-9160.

(15) Shelley, J. C.; Shelley, M. Y.; Reeder, R. C.; Bandyopadhyay, S.; Klein, M. L., A Coarse Grain Model for Phospholipid Simulations. *J. Phys. Chem. B* **2001**, *105* (19), 4464-4470.

(16) Shelley, J. C.; Shelley, M. Y.; Reeder, R. C.; Bandyopadhyay, S.; Moore, P. B.; Klein, M. L., Simulations of Phospholipids Using a Coarse Grain Model. *J. Phys. Chem. B* **2001**, *105* (40), 9785-9792.

(17) Marrink, S. J.; de Vries, A. H.; Mark, A. E., Coarse Grained Model for Semiquantitative Lipid Simulations. *J. Phys. Chem. B* **2003**, *108* (2), 750-760.

(18) Marrink, S. J.; Risselada, H. J.; Yefimov, S.; Tieleman, D. P.; de Vries, A. H., The MARTINI Force Field: Coarse Grained Model for Biomolecular Simulations. *J. Phys. Chem. B* **2007**, *111* (27), 7812-7824.

(19) Izvekov, S.; Voth, G. A., A Multiscale Coarse-Graining Method for Biomolecular Systems. *J. Phys. Chem. B* **2005**, *109* (7), 2469-2473.

(20) Izvekov, S.; Voth, G. A., Multiscale Coarse-Graining of Mixed Phospholipid/Cholesterol Bilayers. *J. Chem. Theory Comput.* **2006**, *2* (3), 637-648.

(21) Orsi, M.; Haubertin, D. Y.; Sanderson, W. E.; Essex, J. W., A Quantitative Coarse-Grain Model for Lipid Bilayers. *J. Phys. Chem. B* **2008**, *112* (3), 802-815.

(22) Orsi, M.; Essex, J. W., The ELBA Force Field for Coarse-Grain Modeling of Lipid Membranes. *PLoS ONE* **2011**, *6* (12), e28637.

(23) Pastor, R. W.; Venable, R. M.; Karplus, M., Model for the Structure of the Lipid Bilayer. *P. Natl. Acad. Sci.* **1991**, *88* (3), 892-896.

(24) Egberts, E.; Marrink, S.-J.; Berendsen, H. J. C., Molecular Dynamics Simulation of a Phospholipid Membrane. *Eur. Biophys. J.* **1994**, *22* (6), 423-436.

(25) Essex, J. W.; Hann, M. M.; Richards, W. G., Molecular Dynamics Simulation of a Hydrated Phospholipid Bilayer. *Philos. T. Roy. Soc. B* **1994**, *344* (1309), 239-260.

(26) Chiu, S. W.; Clark, M.; Balaji, V.; Subramaniam, S.; Scott, H. L.; Jakobsson, E., Incorporation of Surface Tension into Molecular Dynamics Simulation of an Interface: A Fluid Phase Lipid Bilayer Membrane. *Biophys. J.* **1995**, *69* (4), 1230-1245.

(27) Berger, O.; Edholm, O.; Jähnig, F., Molecular Dynamics Simulations of a Fluid Bilayer of Dipalmitoylphosphatidylcholine at Full Hydration, Constant Pressure, and Constant Temperature. *Biophys. J.* **1997**, *72* (5), 2002-2013.

(28) Chandrasekhar, I.; Kastenholz, M.; Lins, R. D.; Oostenbrink, C.; Schuler, L. D.; Tieleman, D. P.; van Gunsteren, W. F., A Consistent Potential Energy Parameter Set for Lipids: Dipalmitoylphosphatidylcholine as a Benchmark of the GROMOS96 45A3 Force Field. *Eur. Biophys. J.* **2003**, *32* (1), 67-77.

(29) Chiu, S.-W.; Pandit, S. A.; Scott, H. L.; Jakobsson, E., An Improved United Atom Force Field for Simulation of Mixed Lipid Bilayers. *J. Phys. Chem. B* **2009**, *113* (9), 2748-2763.

(30) Kukol, A., Lipid Models for United-Atom Molecular Dynamics Simulations of Proteins. *J. Chem. Theory Comput.* **2009**, *5* (3), 615-626.

(31) Poger, D.; van Gunsteren, W. F.; Mark, A. E., A New Force Field for Simulating Phosphatidylcholine Bilayers. *J. Comput. Chem.* **2010**, *31* (6), 1117-1125.

(32) Hénin, J.; Shinoda, W.; Klein, M. L., United-Atom Acyl Chains for CHARMM Phospholipids. *J. Phys. Chem. B* **2008**, *112* (23), 7008-7015.

(33) Lee, S.; Tran, A.; Allsopp, M.; Lim, J. B.; Hénin, J.; Klauda, J. B., CHARMM36 United Atom Chain Model for Lipids and Surfactants. *J. Phys. Chem. B* **2014**, *118* (2), 547-556.

(34) Tjörnhammar, R.; Edholm, O., Reparameterized United Atom Model for Molecular Dynamics Simulations of Gel and Fluid Phosphatidylcholine Bilayers. *J. Chem. Theory Comput.* **2014**, *10* (12), 5706-5715.

(35) McKiernan, K. A.; Wang, L.-P.; Pande, V. S., Training and Validation of a Liquid-Crystalline Phospholipid Bilayer Force Field. *J. Chem. Theory Comput.* **2016**, *12* (12), 5960-5967.

(36) Anézo, C.; de Vries, A. H.; Höltje, H.-D.; Tieleman, D. P.; Marrink, S.-J., Methodological Issues in Lipid Bilayer Simulations. *J. Phys. Chem. B* **2003**, *107* (35), 9424-9433.

(37) Siu, S. W. I.; Vacha, R.; Jungwirth, P.; Böckmann, R. A., Biomolecular Simulations of Membranes: Physical Properties from Different Force Fields. *J. Chem. Phys.* **2008**, *128* (12), 125103.

(38) Hénin, J.; Shinoda, W.; Klein, M. L., Models for Phosphatidylglycerol Lipids Put to a Structural Test. *J. Phys. Chem. B* **2009**, *113* (19), 6958-6963.

(39) Piggot, T. J.; Piñeiro, Á.; Khalid, S., Molecular Dynamics Simulations of Phosphatidylcholine Membranes: A Comparative Force Field Study. *J. Chem. Theory Comput.* **2012**, *8* (11), 4593-4609.

(40) Poger, D.; Mark, A. E., Lipid Bilayers: The Effect of Force Field on Ordering and Dynamics. *J. Chem. Theory Comput.* **2012**, *8* (11), 4807-4817.

(41) Botan, A.; Favela-Rosales, F.; Fuchs, P. F. J.; Javanainen, M.; Kanduč, M.; Kulig, W.; Lamberg, A.; Loison, C.; Lyubartsev, A.; Miettinen, M. S. et al., Toward Atomistic Resolution Structure of Phosphatidylcholine Headgroup and Glycerol Backbone at Different Ambient Conditions. *J. Phys. Chem. B* **2015**, *119* (49), 15075-15088.

(42) Pluhackova, K.; Kirsch, S. A.; Han, J.; Sun, L.; Jiang, Z.; Unruh, T.; Böckmann, R. A., A Critical Comparison of Biomembrane Force Fields: Structure

and Dynamics of Model DMPC, POPC, and POPE Bilayers. *J. Phys. Chem. B* **2016**, *120* (16), 3888-3903.

(43) Seelig, J., Deuterium Magnetic Resonance: Theory and Application to Lipid Membranes. *Q. Rev. Biophys.* **1977**, *10* (3), 353-418.

(44) Seelig, J.; Waespe-Šarčević, N., Molecular Order in Cis and Trans Unsaturated Phospholipid Bilayers. *Biochemistry* **1978**, *17* (16), 3310-3315.

(45) Douliez, J. P.; Léonard, A.; Dufourc, E. J., Restatement of Order Parameters in Biomembranes: Calculation of C-C Bond Order Parameters from C-D Quadrupolar Splittings. *Biophys. J.* **1995**, *68* (5), 1727-1739.

(46) Hong, M.; Schmidt-Rohr, K.; Pines, A., NMR Measurement of Signs and Magnitudes of C-H Dipolar Couplings in Lecithin. *J. Am. Chem. Soc.* **1995**, *117* (11), 3310-3311.

(47) Gross, J. D.; Warschawski, D. E.; Griffin, R. G., Dipolar Recoupling in MAS NMR: A Probe for Segmental Order in Lipid Bilayers. *J. Am. Chem. Soc.* **1997**, *119* (4), 796-802.

(48) Warschawski, D.; Devaux, P., Order Parameters of Unsaturated Phospholipids in Membranes and the Effect of Cholesterol: A 1H–13C Solid-State NMR Study at Natural Abundance. *Eur. Biophys. J.* **2005**, *34* (8), 987-996.

(49) Piggot, T. J.; Piñeiro, Á.; Khalid, S., Correction to Molecular Dynamics Simulations of Phosphatidylcholine Membranes: A Comparative Force Field Study. *J. Chem. Theory Comput.* **2017**.

(50) Vermeer, L. S.; de Groot, B. L.; Réat, V.; Milon, A.; Czaplicki, J., Acyl Chain Order Parameter Profiles in Phospholipid Bilayers: Computation from Molecular Dynamics Simulations and Comparison with 2H NMR Experiments. *Eur. Biophys. J.* **2007**, *36*.

(51) Engel, A. K.; Cowburn, D., The Origin of Multiple Quadrupole Couplings in the Deuterium NMR Spectra of the 2 Chain of 1,2 Dipalmitoyl-sn-glycero-3-phosphorylcholine. *FEBS Lett.* **1981**, *126* (2), 169-171.

(52) Douliez, J.-P.; Ferrarini, A.; Dufourc, E.-J., On the Relationship Between C-C and C-D Order Parameters and its use for Studying the Conformation of Lipid Acyl Chains in Biomembranes. *J. Chem. Phys.* **1998**, *109* (6), 2513-2518.

(53) Van Lehn, R. C.; Alexander-Katz, A., Membrane-Embedded Nanoparticles Induce Lipid Rearrangements Similar to Those Exhibited by Biological Membrane Proteins. *J. Phys. Chem. B* **2014**, *118* (44), 12586-12598.

(54) Gapsys, V.; de Groot, B. L.; Briones, R., Computational Analysis of Local Membrane Properties. *J. Comput. Aided Mol. Des.* **2013**, *27* (10), 845-858.

(55) Pandit, S. A.; Chiu, S.-W.; Jakobsson, E.; Grama, A.; Scott, H. L., Cholesterol Packing around Lipids with Saturated and Unsaturated Chains: A Simulation Study. *Langmuir* **2008**, *24* (13), 6858-6865.

(56) Poger, D.; Mark, A. E., On the Validation of Molecular Dynamics Simulations of Saturated and cis-Monounsaturated Phosphatidylcholine Lipid Bilayers: A Comparison with Experiment. *J. Chem. Theory Comput.* **2009**, *6* (1), 325-336.

(57) Klauda, J. B.; Venable, R. M.; Freites, J. A.; O'Connor, J. W.; Tobias, D. J.; Mondragon-Ramirez, C.; Vorobyov, I.; MacKerell, A. D.; Pastor, R. W., Update

of the CHARMM All-Atom Additive Force Field for Lipids: Validation on Six Lipid Types. *J. Phys. Chem. B* **2010**, *114* (23), 7830-7843.

(58) NMRLipids/MATCH. http://github.com/NMRLipids/MATCH/tree/master/scratch/report (accessed December 2016).

(59) NMRLipids/lipid_ionINTERACTION. http://github.com/NMRLipids/lipid_ionINTERACTION/tree/master/scripts (accessed December 2016).

(60) VMD-L Mailing List. http://www.ks.uiuc.edu/Research/vmd/mailing_list/vmd-l/att-14731/calc_op.tcl (accessed December 2016).

(61) Carr, M.; MacPhee, C. E., Membrainy: A 'Smart', Unified Membrane Analysis Tool. *Source Code Biol. Med.* **2015**, *10* (1), 3.

(62) lipid C-D order parameters using CORREL. http://www.charmm.org/ubbthreads/ubbthreads.php?ubb=showflat&Number=6857&page=1 (accessed December 2016).

(63) Michaud-Agrawal, N.; Denning, E. J.; Woolf, T. B.; Beckstein, O., MDAnalysis: A Toolkit for the Analysis of Molecular Dynamics Simulations. *J. Comput. Chem.* **2011**, *32* (10), 2319-2327.

(64) Guixà-González, R.; Rodriguez-Espigares, I.; Ramírez-Anguita, J. M.; Carrió-Gaspar, P.; Martinez-Seara, H.; Giorgino, T.; Selent, J., MEMBPLUGIN: Studying Membrane Complexity in VMD. *Bioinformatics* **2014**, *30* (10), 1478-1480.

(65) Jeong, J. C.; Jo, S.; Wu, E. L.; Qi, Y.; Monje-Galvan, V.; Yeom, M. S.; Gorenstein, L.; Chen, F.; Klauda, J. B.; Im, W., ST-analyzer: A Web-Based User Interface for Simulation Trajectory Analysis. *J. Comput. Chem.* **2014**, *35* (12), 957-963.

(66) [gmx-users] Calculation of unsaturated deuterium order parameters for POPC. http://www.mail-archive.com/gmx-users@gromacs.org/msg41543.html (accessed December 2016).

(67) Bug #1166: g_order is incorrect for unsaturated carbons - GROMACS - Gromacs development. http://redmine.gromacs.org/issues/1166 (accessed December 2016).

(68) The NMRlipids project. http://nmrlipids.blogspot.co.uk/ (accessed December 2016).

(69) Nmrlipids. http://zenodo.org/communities/nmrlipids/?page=1&size=20 (accessed December 2016).

(70) Jämbeck, J. P. M.; Lyubartsev, A. P., An Extension and Further Validation of an All-Atomistic Force Field for Biological Membranes. *J. Chem. Theory Comput.* **2012**, *8* (8), 2938-2948.

(71) Maciejewski, A.; Pasenkiewicz-Gierula, M.; Cramariuc, O.; Vattulainen, I.; Rog, T., Refined OPLS All-Atom Force Field for Saturated Phosphatidylcholine Bilayers at Full Hydration. *J. Phys. Chem. B* **2014**, *118* (17), 4571-4581.

(72) Kulig, W.; Jurkiewicz, P.; Olżyńskab, A.; Tynkkynen, J.; Javanainen, M.; Manna, M.; Rog, T.; Hof, M.; Vattulainen, I.; Jungwirth, P., Experimental Determination and Computational Interpretation of Biophysical Properties of Lipid

Bilayers Enriched by Cholesteryl Hemisuccinate. *BBA - Biomembranes* **2015**, *1848* (2), 422-432.

(73) Kulig, W.; Pasenkiewicz-Gierula, M.; Róg, T., Cis and Trans Unsaturated Phosphatidylcholine Bilayers: A Molecular Dynamics Simulation Study. *Chem. Phys. Lipids* **2016**, *195*, 12-20.

(74) POPC @ 310K, model by Maciejewski and Rog. http://doi.org/10.5281/zenodo.13497 (accessed January 2017).

(75) Abraham, M. J.; Murtola, T.; Schulz, R.; Páll, S.; Smith, J. C.; Hess, B.; Lindahl, E., GROMACS: High Performance Molecular Simulations Through Multi-Level Parallelism from Laptops to Supercomputers. *SoftwareX* **2015**, *1-2*, 19-25.

(76) Hess, B., P-LINCS: A Parallel Linear Constraint Solver for Molecular Simulation. *J. Chem. Theory Comput.* **2007**, *4* (1), 116-122.

(77) Nosé, S., A Molecular Dynamics Method for Simulations in the Canonical Ensemble. *Mol. Phys.* **1984**, *52* (2), 255-268.

(78) Hoover, W. G., Canonical Dynamics: Equilibrium Phase-Space Distributions. *Phys. Rev. A* **1985**, *31* (3), 1695-1697.

(79) Parrinello, M.; Rahman, A., Polymorphic Transitions in Single Crystals: A New Molecular Dynamics Method. *J. Appl. Phys.* **1981**, *52* (12), 7182-7190.

(80) Nosé, S.; Klein, M. L., Constant Pressure Molecular Dynamics for Molecular Systems. *Mol. Phys.* **1983**, *50* (5), 1055-1076.

(81) Lindorff-Larsen, K.; Piana, S.; Palmo, K.; Maragakis, P.; Klepeis, J. L.; Dror, R. O.; Shaw, D. E., Improved Side-Chain Torsion Potentials for the Amber ff99SB Protein Force Field. *Proteins* **2010**, *78* (8), 1950-1958.

(82) Essmann, U.; Perera, L.; Berkowitz, M.; Darden, T.; Lee, H.; Pedersen, L., A Smooth Particle Mesh Ewald Method. *J. Chem. Phys.* **1995**, *103* (19), 8577-8593.

(83) Páll, S.; Hess, B., A Flexible Algorithm for Calculating Pair Interactions on SIMD Architectures. *Comput. Phys. Commun.* **2013**, *184* (12), 2641-2650.

(84) Jorgensen, W. L.; Chandrasekhar, J.; Madura, J. D.; Impey, R. W.; Klein, M. L., Comparison of Simple Potential Functions for Simulating Liquid Water. *J. Chem. Phys.* **1983**, *79* (2), 926-935.

(85) Ulmschneider, J. P.; Ulmschneider, M. B., United Atom Lipid Parameters for Combination with the Optimized Potentials for Liquid Simulations All-Atom Force Field. *J. Chem. Theory Comput.* **2009**, *5* (7), 1803-1813.

(86) Lee, J.; Cheng, X.; Swails, J. M.; Yeom, M. S.; Eastman, P. K.; Lemkul, J. A.; Wei, S.; Buckner, J.; Jeong, J. C.; Qi, Y. et al., CHARMM-GUI Input Generator for NAMD, GROMACS, AMBER, OpenMM, and CHARMM/OpenMM Simulations Using the CHARMM36 Additive Force Field. *J. Chem. Theory Comput.* **2016**, *12* (1), 405-413.

(87) Durell, S. R.; Brooks, B. R.; Ben-Naim, A., Solvent-Induced Forces between Two Hydrophilic Groups. *J. Phys. Chem-US* **1994**, *98* (8), 2198-2202.

(88) Neria, E.; Fischer, S.; Karplus, M., Simulation of Activation Free Energies in Molecular Systems. *J. Chem. Phys.* **1996**, *105* (5), 1902-1921.

(89) POPC_Ulmschneider_OPLS_Verlet_Group. http://doi.org/10.5281/zenodo.30904 (accessed May 2016).

(90) Domański, J.; Stansfeld, P.; Sansom, M.; Beckstein, O., Lipidbook: A Public Repository for Force-Field Parameters Used in Membrane Simulations. *J. Membrane Biol.* **2010**, *236* (3), 255-258.

(91) Ulmschneider results for POPC without ions · Issue #8 · NMRLipids/lipid_ionINTERACTION. http://github.com/NMRLipids/lipid_ionINTERACTION/issues/8 (accessed December 2016).

(92) Bachar, M.; Brunelle, P.; Tieleman, D. P.; Rauk, A., Molecular Dynamics Simulation of a Polyunsaturated Lipid Bilayer Susceptible to Lipid Peroxidation. *J. Phys. Chem. B* **2004**, *108* (22), 7170-7179.

(93) Ollila, S.; Hyvönen, M. T.; Vattulainen, I., Polyunsaturation in Lipid Membranes: Dynamic Properties and Lateral Pressure Profiles. *J. Phys. Chem. B* **2007**, *111* (12), 3139-3150.

(94) MD simulation trajectory and related files for POPC bilayer (Berger model delivered by Tieleman, Gromacs 4.5). http://doi.org/10.5281/zenodo.13279 (accessed January 2017).

(95) Ferreira, T. M.; Coreta-Gomes, F.; Ollila, O. H. S.; Moreno, M. J.; Vaz, W. L. C.; Topgaard, D., Cholesterol and POPC Segmental Order Parameters in Lipid Membranes: Solid State 1H-13C NMR and MD Simulation Studies. *Phys. Chem. Chem. Phys.* **2013**, *15* (6), 1976-1989.

(96) Seelig, J.; Seelig, A., Lipid Conformation in Model Membranes and Biological Membranes. *Q. Rev. Biophys.* **1980**, *13* (1), 19-61.

(97) Gally, H. U.; Pluschke, G.; Overath, P.; Seelig, J., Structure of *Escherichia coli* Membranes. Phospholipid Conformation in Model Membranes and Cells as Studied by Deuterium Magnetic Resonance. *Biochemistry* **1979**, *18* (25), 5605-5610.

(98) Rance, M.; Jeffrey, K. R.; Tulloch, A. P.; Butler, K. W.; Smith, I. C. P., Orientational Order of Unsaturated Lipids in the Membranes of *Acholeplasma laidlawii* as Observed by 2H-NMR. *BBA - Biomembranes* **1980**, *600* (2), 245-262.

(99) Browning, J. L.; Seelig, J., Bilayers of Phosphatidylserine: A Deuterium and Phosphorus Nuclear Magnetic Resonance Study. *Biochemistry* **1980**, *19* (6), 1262-1270.

(100) Seelig, J.; Browning, J. L., General Features of Phospholipid Conformation in Membranes. *FEBS Lett.* **1978**, *92* (1), 41-44.

(101) Ollila, O. H. S.; Pabst, G., Atomistic Resolution Structure and Dynamics of Lipid Bilayers in Simulations and Experiments. *BBA - Biomembranes* **2016**, *1858* (10), 2512-2528.

(102) Pastor, R. W.; MacKerell, A. D., Development of the CHARMM Force Field for Lipids. *J. Phys. Chem. Lett.* **2011**, *2* (13), 1526-1532.

(103) Kruczek, J.; Chiu, S.-W.; Jakobsson, E.; Pandit, S. A., Effects of Lithium and Other Monovalent Ions on Palmitoyl Oleoyl Phosphatidylcholine Bilayer. *Langmuir* **2017**, *33* (4), 1105-1115.

TOC Graphic

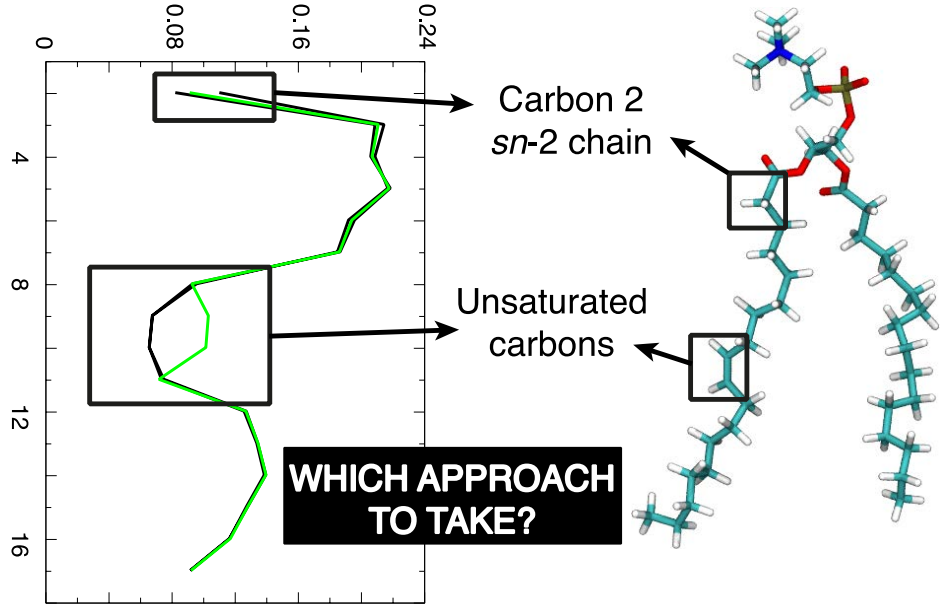
0.08
0.16
0.24
0
4
8
12
16
Carbon 2
sn-2 chain
Unsaturated
carbons
WHICH APPROACH
TO TAKE?